ORIGINAL PAPER

RJME
Romanian Journal of Morphology & Embryology
http://www.rjme.ro/

Correlations between intratumoral vascular network and tumoral architecture in prostatic adenocarcinoma

I. E. PLEŞEA[1)], A. STOICULESCU[1,2)], M. ŞERBĂNESCU[1)], D. O. ALEXANDRU[3)], M. MAN[4)], O. T. POP[5)], R. M. PLEŞEA[1)]

[1)]*Department of Pathology, University of Medicine and Pharmacy of Craiova*
[2)]*Department of Urology, Emergency County Hospital, Pitesti*
[3)]*Department of Informatics, University of Medicine and Pharmacy of Craiova*
[4)]*Department of Pathology, Emergency County Hospital, Pitesti*
[5)]*Research Center for Microscopic Morphology and Immunology, University of Medicine and Pharmacy of Craiova*

Abstract

The authors made a preliminary assessment of possible correlations between the intratumoral vascular density (IVD) and the architectural tumoral patterns described by Gleason. The studied material consisted of samples obtained by transurethral resection from 34 patients diagnosed with prostatic adenocarcinoma. Ten fields, five for dominant and five for secondary identified patterns of each case, with no necrosis were selected randomly from CD34 immunomarked sections using ×20 objective. IVD increased with Gleason pattern both for the entire group, but also for "solid" phenotype group of subtypes up to pattern 4, respectively subtype 4B. In "necrotizing" phenotype group of subtypes, IVD had a decreasing trend from the better-differentiated subtypes to the poorest one. These preliminary data showed that the intratumoral vascular network reacts differently to the loss of tumoral differentiation in the two groups of Gleason subtypes suggesting the existence of two different populations of malignant cells.

Keywords: prostate carcinoma, Gleason pattern, vascular density.

Introduction

Tumoral stroma could be defined as the whole of modified mesenchymal structures that support the malignant tissue. As both supporting scaffold and nutritional system, tumoral stroma accompanies any neoplastic proliferation, being better distributed and observed in carcinomas rather than in sarcomas, in the latter being identified with difficulty. It represents a reaction of connective tissue which undergoes different changes in contact with tumoral parenchyma and thus comprises newly formed elements but which are non-tumoral [1, 2].

The ratio between supporting connective–vascular structure and the whole of malignant cells forming the tumoral parenchyma varies considerably in different types of malignant tumors, the reasons of this variation remaining still unclear. When a tissue is growing or a primary tumor is developing, the exceeding of a certain dimension (2–4 mm^3) requires an optimal inflow of oxygen and an on outflow of cellular waste products [3]. The growth of new blood vessels is necessary for sustaining the increased metabolic needs of a larger cellular population and is realized by activation of already existing vascular bed. Thus, angiogenesis plays an essential role in the stability of normal or modified epithelia and their supporting interstitial matrix.

The proliferating and invasive tumoral cells may induce numerous answers in the mesenchymal vascular network. These changes in the angiogenic activity are due to the production of factors responsible for the initiation of angiogenesis, which results in the developing of newly formed vessels [4].

In prostate cancer, an important, supporting and/or inhibiting role of stromal–epithelial interactions has been implicated in tumor growth, angiogenesis and metastasis, which includes cell proliferation, adhesion and motility [5]. One of the essential events with morphological expression of prostatic malignant tissue "reactive stroma" – concept defined since 1998 [6] and proved to be responsible for the genesis, development, invasion, progression and tumor metastasis [7] – is the amplification of angiogenesis [8].

Despite the consistent number of studies in the literature of the last decades focused on the interactions between tumoral stroma of prostatic cancer and its population of malignant cells, only few of them address the quantitative relationship between intratumoral vascular density and tumor parenchyma.

The present study is part of a larger project investigating the possible correlations between the different intratumoral stromal components, as interstitial fibrillary network [9] and vascular network and the architectural tumoral patterns described by Gleason and aims to analyze the relationship between the density of the vascular network within the tumor microenvironment and the degree of differentiation of tumor parenchyma in prostate carcinoma assessed using the Gleason system.

Materials and Methods

The studied group includes 34 patients admitted with suspected nodular benign prostatic hyperplasia (NBH) and no specific previous treatment who underwent trans-urethral resection (TURP), in whom the postoperative histopathological examination established the incidental presence of malignant carcinomatous proliferation invading the NBH area.

In addition to the five serial sections made from the paraffin blocks containing the prostate tissue fragments collected by TURP and stained with HE (first section), for setting the Gleason patterns and with special stains for connective tissue (sections 2–5) for the qualitative assessment of intratumoral stromal fibrillary compound, a sixth section was cut, placed on SuperFrost® slides and immunomarked with monoclonal anti-CD34 antibody, QBEnd 10 clone (DAKO) with a dilution of 1:50, after previous application of three-stage indirect Steptavidin–Biotin Complex (SaBC)/Horseradish peroxidase (HRP) method. DAB chromogen and Hematoxylin counterstaining were used for visualization of intratumoral vascular structures. As for the assessment of intratumoral vascular density, two main architectural patterns: the dominant pattern and the secondary one were assessed for each of the 34 cases and then, five randomly selected fields without necrosis at ×20 magnification were selected for each pattern, so as to each case 10 tumor areas were selected. Thus, the final batch was composed of 340 tumor areas, which were assigned to the five main groups of tumor architectural aspects described by Gleason and their variants, which were distributed as in the Figure 1.

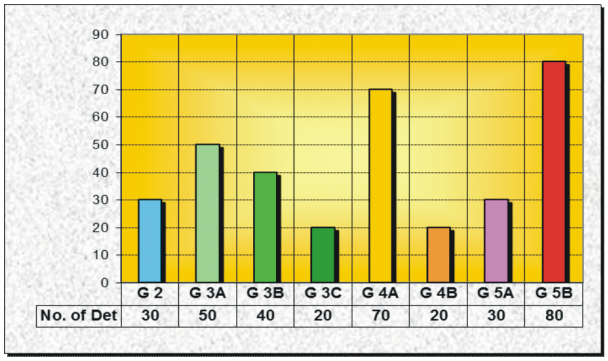

Figure 1 – ***Distribution of determinations according to Gleason subtypes.***

Two additional groups were designed, according to Gleason diagram of pattern subtypes:

- the "necrotizing phenotype" group, including the subtypes 3C, 4A and 5A, in which tumoral proliferation seems to evolve towards solid individual masses with central necrosis, passing through a cribriform stage;
- the "solid phenotype" group, including the subtypes 3A, 3B, 4B and 5B in which tumoral proliferation seems to evolve from well-differentiated glandular aspects of pattern 2 towards solid variable clusters of undifferentiated tumoral cells of 5B subtype.

Quantitative morphometric measurements of intra-tumoral vascular densities (IVD) were performed using the "Measurements" module of the Analysis Pro 5.0 software. Values were grouped into four classes for the stromal component density score, shown in Table 1.

Table 1 – ***Scale of VD values***

Score	Vascular Density – IVD (capillaries/mm^2)
VD 1	<100
VD 2	100–200
VD 3	200–300
VD 4	>300

The lowest value (VMIN), the highest value (VMAX), the half range value (HRV), mean value (AV), standard deviation (STDEV) were assessed for each pattern.

Student *t*-test was used to compare vascular density mean values of different Gleason patterns and subtypes, Kolmogorov–Smirnov test was used to compare vascular density values distributions of different Gleason patterns and subtypes, and χ^2 test was used to compare vascular density values divided into score classes in different Gleason patterns and subtypes.

Results

General assessment

The intratumoral vascular density varied within wide ranges of values, whose lowest limit (28.94 capillaries/mm^2) was observed in the pattern 5 group of samples, and highest limit in the pattern 4 group of samples (674.78 capillaries/mm^2). The largest range was observed in the pattern 5 group of samples (Table 2; Figures 2 and 3).

Table 2 – ***Distribution of main statistical parameters in Gleason patterns***

Parameter	Value			
	Gleason 2	*Gleason 3*	*Gleason 4*	*Gleason 5*
No. of samples	30	110	90	110
VMIN	59.54	19.85	79.39	28.94
VMAX	357.24	476.32	674.78	575.55
HRV	208.39	248.08	377.08	302.24
AV	**138.92**	**211.09**	**293.95**	**248.63**
STDEV	68.55	99.64	126.57	131.13
AV + STDEV	207.48	310.73	420.52	379.76
AV - STDEV	70.37	111.45	167.38	117.5

In spite of this dispersion, in all pattern groups, most values were grouped in ranges of smaller amplitudes, determined by variable values of STDEV around the each group AV value. In all the pattern groups, the AV value of VD had a smaller value than the corresponding HRV, the intervals including the majority of values being thus displaced towards the lower limit of the ranges (Table 2; Figure 2).

The most interesting observation was that AV values had a decrease in pattern 5, after an ascending trend from pattern 2 to pattern 4 (Table 2; Figure 2).

The statistical comparison between IVD mean values of Gleason main groups using Student *t*-test, underlined the differences between them (Table 3), differences clearly illustrated also in Figure 2.

Table 3 – ***Statistical comparison between IVD mean values in Gleason patterns***

Student *t*-test	Gleason 2	Gleason 3	Gleason 4
Gleason 2			
Gleason 3	0.0002		
Gleason 4	<0.0001	<0.0001	
Gleason 5	<0.0001	0.018 (<0.05)	0.014 (<0.05)

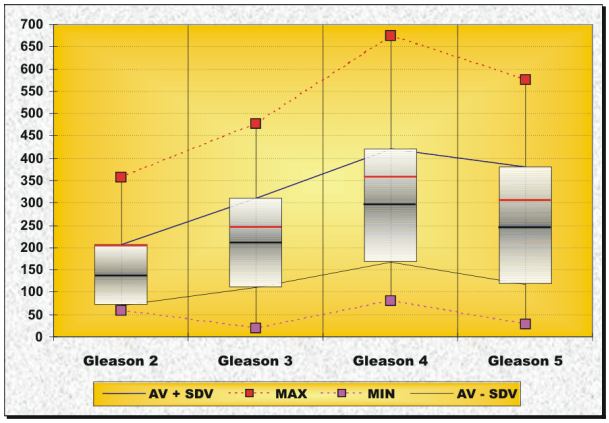

Figure 2 – ***Comparative representation of IVD main statistical parameters in Gleason patterns.***

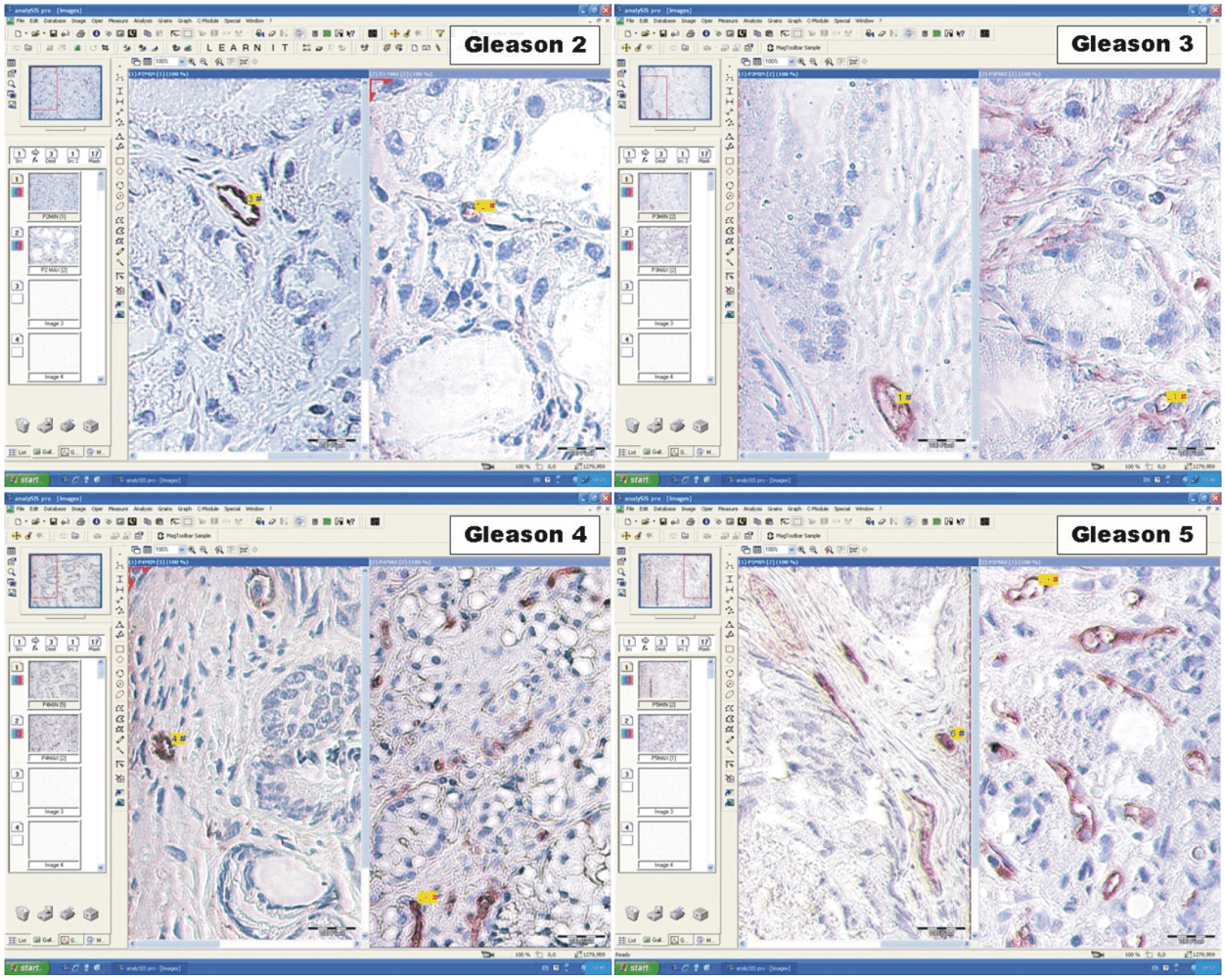

Figure 3 – ***The windows of image analysis program showing the IVD lowest and highest values in Gleason groups.***

The analysis of the main statistical parameters in the subtypes of Gleason patterns from 3 to 5 revealed some interesting aspects. A wide dispersion of values was noticed only in 5B subtype of pattern 5. The intervals comprising the majority of values (as defined by the STDEVs around AVs) were generally more "condensed" than the corresponding ranges and were almost similar, excepting Gleason 4B and 5B subtypes which had wider limits than the others (Figure 4).

In pattern 3 subtypes, these intervals had almost the same wideness and were all displaced towards the lower limit of the corresponding ranges because AVs of IVD were, in all subtypes of pattern 3, were smaller than the corresponding HRV-s (Figures 4 and 5). The IVD values have an overall ascending trend from 3A subtype to 3C subtype, more obvious between 3A subtype and 3B subtype and smoother between 3B subtype and 3C subtype. This trend was confirmed by the statistical comparison between IVD mean values of Gleason 3 subtypes using Student test, which showed, on one hand, the differences between the AVs of 3A and 3B subtypes and 3A and 3C subtypes and, on the other hand, underlined the similarity between the AVs of 3B and 3C subtypes (Table 4).

Parameter	Value						
	GL 3A	GL 3B	GL 3C	GL 4A	GL 4B	GL 5A	GL 5B
No. Samples	50	40	20	70	20	30	80
VMIN	19,85	79,39	119,08	79,39	277,85	28,94	59,54
VMAX	396,93	476,32	436,62	476,32	674,78	337,39	575,55
HRV	208,39	277,85	277,85	277,85	476,31	183,64	317,54
AV	167,11	245,60	252,05	245,81	462,42	134,33	291,50
STDEV	86,1	92,84	103,85	75,57	126,03	91,25	117,67
AV + STDEV	253,2	338,44	355,9	321,39	588,45	225,58	409,168
AV - STDEV	81,01	152,76	148,2	170,24	336,39	43,083	173,82

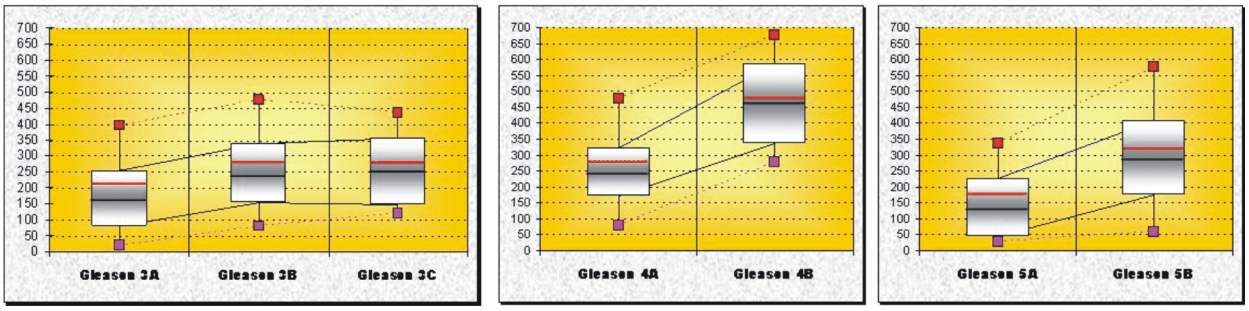

Figure 4 – ***Distribution and comparative representation of IVD main statistical parameters in Gleason subgroups.***

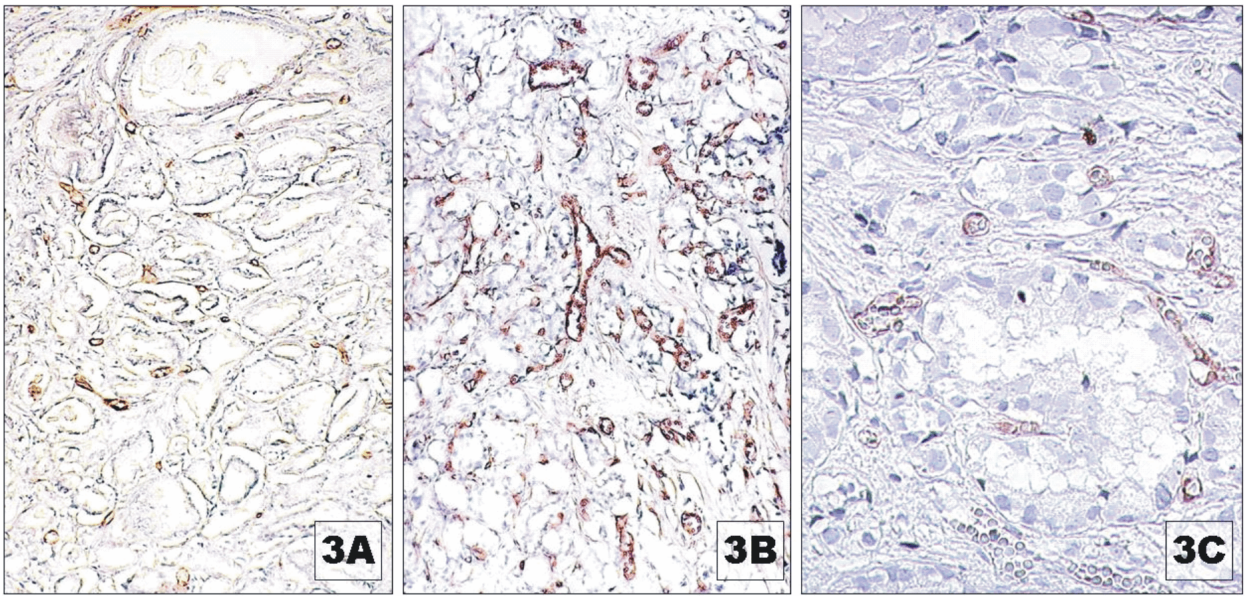

Figure 5 – ***Different aspects of tumoral vascular network in pattern Gleason 3 subtypes.***

Table 4 – ***Statistical comparison between IVD mean values in Gleason pattern subtypes***

Student *t*-test	Gleason 3A	Gleason 3B	Gleason 4B	Gleason 5B
Gleason 3A				
Gleason 3B	**<0.0001**			
Gleason 3C	**0.001** (<0.05)	0.808 (>0.05)		
Gleason 4A			**<0.0001**	
Gleason 5A				**<0.0001**

In pattern 4, the IVD expressed different distributions in the two subtypes. Thus, although the whole ranges of values were similar in length, in subtype 4a, the interval comprising the majority of values was more "condensed" around an AV value smaller than the corresponding HRV which displaced the interval on the lower limit of the range, whereas in subtype 4B the same interval was larger and the AV value, higher than that of the former subgroup, but smaller and almost equal to the HRV placed the interval comprising the majority of values very close to the middle of the whole range (Figures 4 and 6).

The statistical comparison of the AVs of Gleason 4 subtypes using Student *t*-test, confirmed the evident difference between them (Table 4).

In pattern 5, the IVD had also different models of distribution in its two subtypes. Thus, in subtype 5a, the whole range of values was smaller, the interval comprising the majority of values was more "condensed" around an AV smaller than the corresponding HRV which displaced the interval towards the lower limit of the range, whereas

in subtype 5B, both the whole range and the interval comprising the majority of values were larger and the AV, higher than that of the former subgroup, was although smaller than the corresponding HRV (Figures 4 and 7).

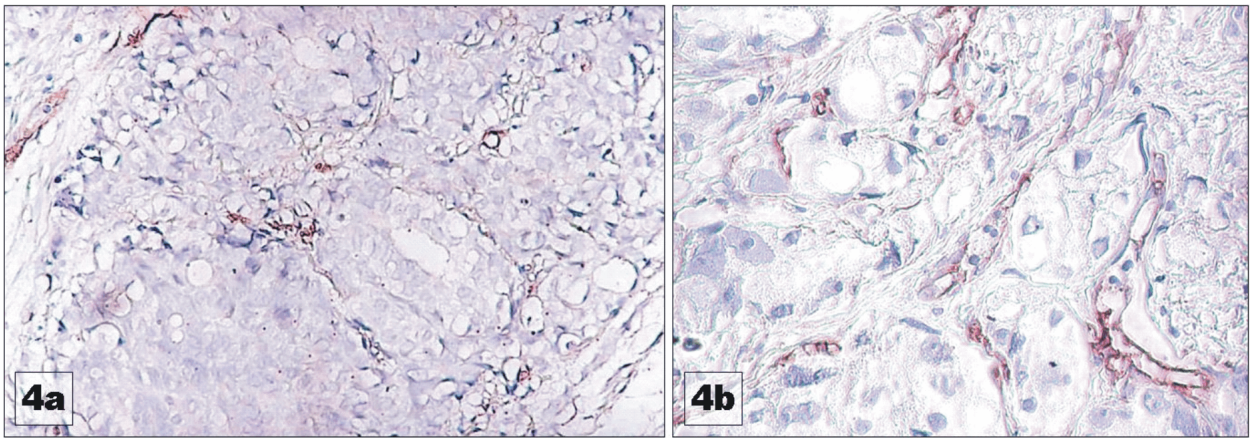

Figure 6 – ***Different aspects of tumoral vascular network in pattern Gleason 4 subtypes.***

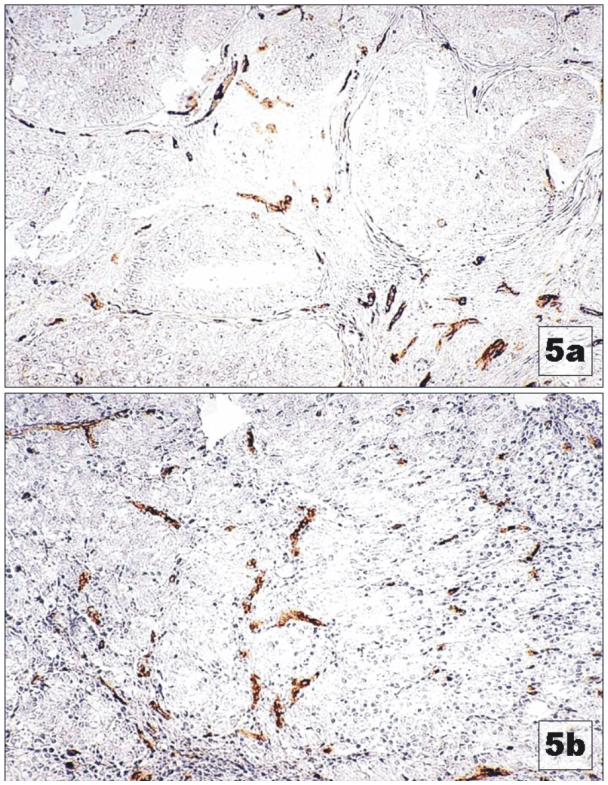

Figure 7 – ***Different aspects of tumoral vascular network in pattern Gleason 4 subtypes.***

The statistical comparison of the AVs of Gleason 5 subtypes using Student *t*-test, confirmed the evident difference between them (Table 4).

Finally, if we follow the AVs from subgroup 3A to subgroup 5B we can observe that they have a smooth ascending trend from 3A subtype to 4B subtype which has a small "gap" in the 4A subtype, where the AV value of the IVD is smaller than that of the 3c subtype (Figure 4) and we have to notice the evident "gap" in 5A subtype, whose AV is smaller even than that of 3A subtype.

"Necrotizing" phenotype

In the "necrotizing" phenotype group, there are several aspects revealed by the analysis of the main statistical parameters. The first one is that there are no striking differences between the lengths of subtypes' whole ranges. The second important aspect is that all AVs are smaller than their corresponding HRVs so that all intervals comprising the majority of values are displaced towards the lower limits of the whole ranges. The third aspect to be noticed is the descending trend of AVs from the better-differentiated subtype to the poorest one. This trend is very smooth from 3C subtype to 4A subtype and becomes evident towards the 5A subtype (Table 5; Figure 8).

Table 5 – ***Distribution of IVD main statistical parameters in subtypes of "necrotizing" phenotype***

Parameter	Value		
	Gleason 3c	*Gleason 4a*	*Gleason 5a*
No. of samples	20	70	30
VMIN	119.08	79.39	28.94
VMAX	436.62	476.32	337.39
HRV	277.85	277.85	183.64
AV	252.05	245.81	134.33
STDEV	**103.85**	**75.57**	**91.25**
AV + STDEV	355.9	321.39	225.58
AV - STDEV	148.2	170.24	43.083

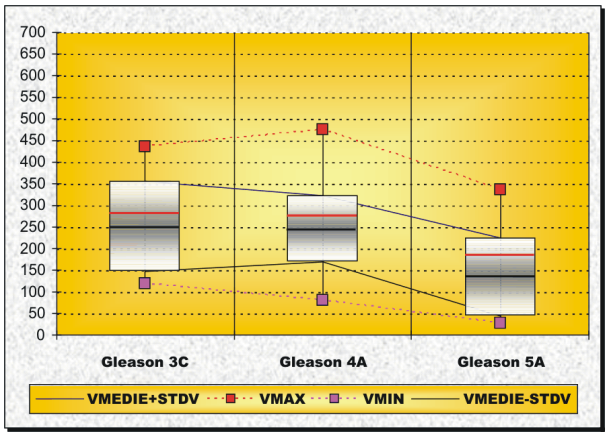

Figure 8 – ***Comparative representation of IVD main statistical parameters in subtypes of "necrotizing" phenotype.***

The statistical comparison of the AVs of "necrotizing" phenotype subtypes using Student *t*-test, confirmed the above-mentioned trend (Table 6).

Table 6 – *Statistical comparison between IVD mean values in subtypes of "necrotizing" phenotype*

Student *t*-test	Gleason 3c	Gleason 4a
Gleason 3c		
Gleason 4a	**0.766** (>0.05)	
Gleason 5a	**0.0001**	**<0.0001**

"Solid" phenotype

In the "solid" phenotype subtypes, the situation is totally different in some points of view from the one described above.

Whole ranges have similar lengths, excepting that of 5B subtype, which is the largest. The intervals comprising the majority of values were splitted in two groups according to their length: the pattern 3 subtypes, with STDEVs around "90", and, consequently more condensed ranges around AVs and the poorly differentiated subtypes, with a STDEV around "120" and, consequently, larger ranges around AVs. As in "necrotizing" phenotype group, all AVs of "solid" phenotype group are smaller than their corresponding HRVs so that all intervals comprising the majority of values are all displaced towards the lower limits of the whole ranges (Table 7; Figure 9).

The difference between the two phenotypes is represented by the trend of AVs. In "solid" phenotype, this trend is somehow similar to that observed above in Gleason patterns but more pronounced.

Table 7 – *Distribution of IVD main statistical parameters in subtypes of "solid" phenotype*

Parameter	Value			
	Gleason 3a	*Gleason 3b*	*Gleason 4b*	*Gleason 5b*
No. of samples	50	40	20	80
VMIN	19.85	79.39	277.85	59.54
VMAX	396.93	476.32	674.78	575.55
HRV	208.39	277.85	476.31	317.54
AV	**167.11**	**245.6**	**462.42**	**291.5**
STDEV	86.1	92.84	126.03	117.67
AV + STDEV	253.2	338.44	588.45	409.168
AV - STDEV	81.01	152.76	336.39	173.82

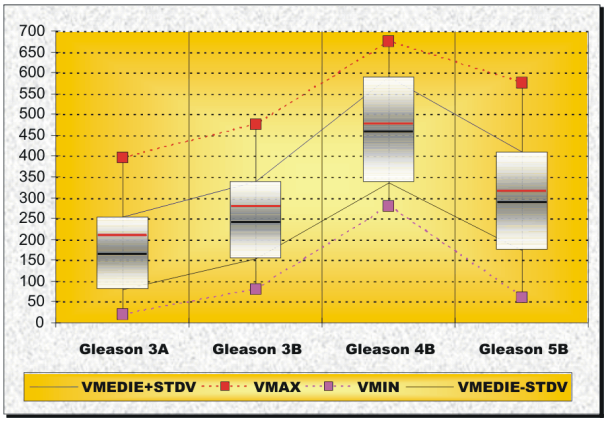

Figure 9 – *Comparative representation of IVD main statistical parameters in subtypes of "solid" phenotype.*

Thus, there is an obvious ascending trend of AVs from 3A subtype towards 4B subtype, followed by a clear breakdown in 5B subtype all these differences between AVs being confirmed by the statistical comparison using Student *t*-test (Table 8).

Table 8 – *Statistical comparison between IVD mean values in subtypes of "solid" phenotype*

Student *t*-test	Gleason 3a	Gleason 3b	Gleason 4b
Gleason 3a			
Gleason 3b	**<0.0001**		
Gleason 4b	**<0.0001**	**<0.0001**	
Gleason 5b	**<0.0001**	**0.033** (<0.05)	**<0.0001**

Discussion

Tumors have been shown to be heterogeneous in the ability of their individual tumor cells to be angiogenic. Therefore, the vascular density is variable in different tumors, and even in different foci of the same tumor [10]. Intratumoral vascular density is considered by many authors to be a marker of the neo-angiogenetic process, which, in turn, was proved to play a pivotal role in neoplastic processes, being responsible, for tumor growth, progression and metastasis spread [11–18]. Thus, quantification of angiogenesis has been demonstrated to provide prognostic information in different human neoplasms [19–26].

The reports in the literature are controversial concerning the role of vascular density as prognostic indicator in prostatic carcinoma [18]. However, there are authors that consider that determination of micro-vessel density in primary prostate carcinoma is an independent predictor of tumor progression [27, 28].

General assessment

There were significant differences between distributions of the IVD values in the main pattern of Gleason system, fact confirmed by the comparative statistical analysis (Table 9).

Table 9 – *P-values of Kolmogorov–Smirnov (K–S) test comparison between distributions of IVD values in Gleason patterns*

K–S test	Gleason 2	Gleason 3	Gleason 4
Gleason 2			
Gleason 3	**0.0001**		
Gleason 4	**<0.0001**	**<0.0001**	
Gleason 5	**<0.0001**	**0.005** (<0.05)	**0.001** (<0.05)

Moreover, the IVD had, to a point, an overall increasing trend from well-differentiated patterns towards poorly differentiated ones. Thus, while more than 90% of pattern 2 areas had a IVD smaller than 200 capillaries/mm^2, in 75% of pattern 4 areas the IVD was higher than 200 capillaries/mm^2 (Table 10; Figure 10, a and b). However, in pattern 5 areas, the above-mentioned trend was "broken" by a more heterogeneous, non-polarized distribution (Figure 10b).

Table 10 – *P-values of χ^2 test comparison between distributions of IVD classes in Gleason patterns*

χ^2 test	Gleason 2	Gleason 3	Gleason 4	General
Gleason 2				
Gleason 3	**0.001**			
Gleason 4	**<0.0001**	**<0.0001**		
Gleason 5	**<0.0001**	**0.019**	**0.004**	
General				**<0.0001**

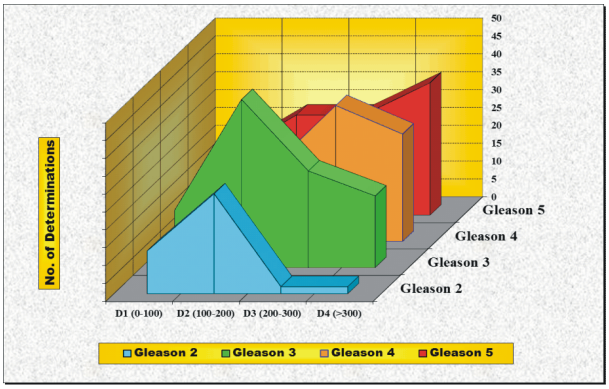

Figure 10a – ***Graphic representation of different IVD ratio values distributions in Gleason patterns.***

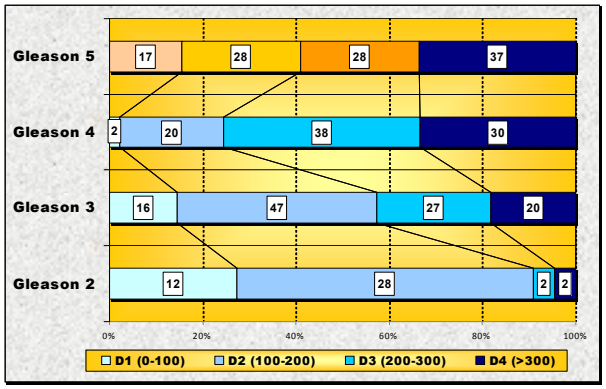

Figure 10b – ***Graphic representation of different IVD ratio classes proportions in Gleason patterns.***

Our data correspond to a point with those of the literature which mention that there is a statistically significant increase in the IVD in the premalignant and malignant tissues in comparison with normal prostatic glands, with a significantly decreased heterogeneity in tumor vasculature as compared to normal prostate [10, 29] and, moreover, the IVD is strongly related to tumor grade expressed also by Gleason system [10, 13, 17, 30, 31], meaning that poorly differentiated adenocarcinomas have a higher IVD than well-differentiated tumors [10, 18] although Montironi R *et al.* demonstrated an increased capillary density in the PIN areas compared to the adenocarcinoma [32].

In each Gleason pattern starting from "3", the IVD had different distributions in the corresponding subtypes, fact confirmed by the statistical comparative analysis (Table 11; Figure 11).

Thus, in pattern 3, there was an increasing trend of IVD from subtype "A" to subtype "C", "smoothed" between subtypes "B" and "C". The same increasing trend was observed in patterns 4 and 5 too from subtypes "A" to subtypes "B" but more pronounced. It is interesting to note that, whereas in pattern 3 the increasing trend is from "solid" subtypes to "necrotizing" subtype, in patterns 4 and 5, the trend is inverse, *i.e.*, from "solid" subtypes to "necrotizing" subtypes (Table 12; Figure 12).

It seems that the most vascularized subtype is "4B" and the least vascularized one is "5A" (Figure 12).

K-S Test	Gleason 3A	Gleason 3B	Gleason 4B	Gleason 5B
Gleason 3A				
Gleason 3B	0,0002			
Gleason 3C	0,032 (< 0,05)	0,920 (> 0,05)		
Gleason 4A			< 0,0001	
Gleason 5A				< 0,0001

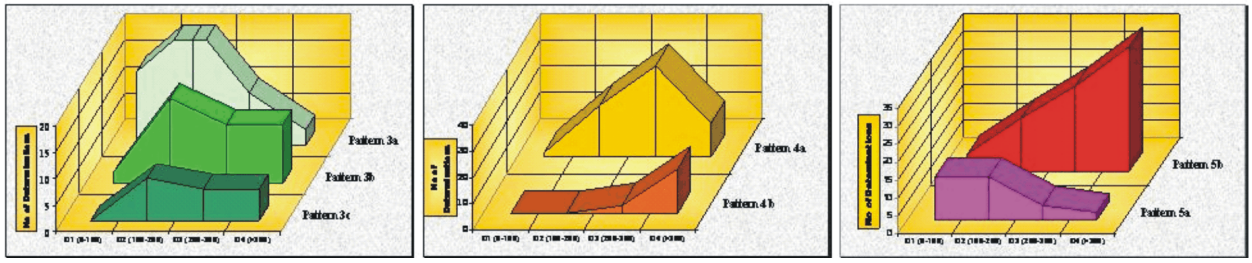

Table 11 and Figure 11 – ***P-values of K–S test comparison between distributions of IVD values in Gleason subtypes and graphic representation of these distributions.***

χ^2 Test	Gleason 3a	Gleason 3b	Gleason 4b	Gleason 5b
Gleason 3a				
Gleason 3b	0,003			
Gleason 3c	0,005	0,787 (> 0,05)		
Gleason 4a			< 0,0001	
Gleason 5a				< 0,0001

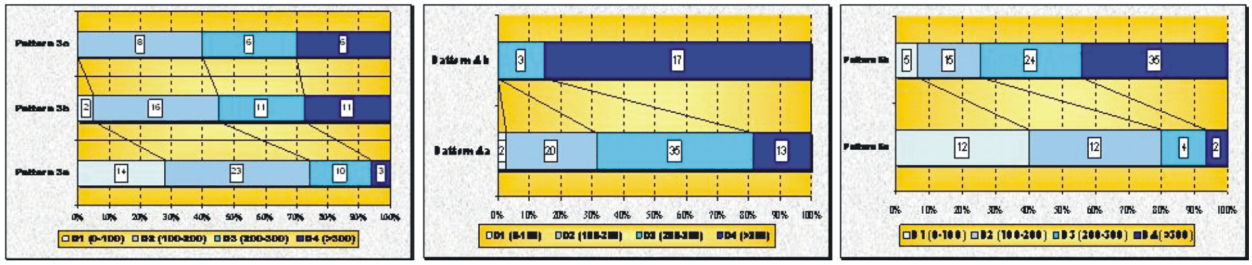

Table 12 and Figure 12 – ***P-values of $\chi 2$ test comparison between distributions of IVD ratio classes in Gleason subtypes and graphic representation of these proportions.***

"Necrotizing" phenotype

It is a clear statistically proved difference between IVD distributions of better differentiated subtypes 3C and 4A and the poorest differentiated subtype 5A of "necrotizing" group of subtypes but no difference between 3C and 4A subtypes (Table 13; Figure 13).

Table 13 – *P-values of K–S test comparison between distributions of IVD values in "necrotizing" phenotype group of patterns*

K–S test	Gleason 3C	Gleason 4A
Gleason 3C		
Gleason 4A	**0.543** (>0.05)	
Gleason 5A	**0.005** (<0.05)	**<0.0001**

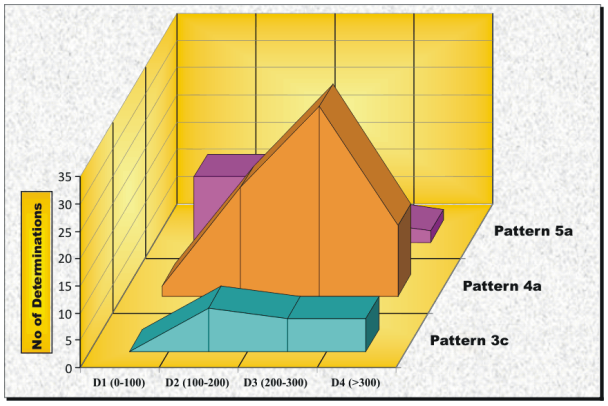

Figure 13 – *Graphic representation of different IVD ratio values distributions in "necrotizing" phenotype.*

What the trend of AVs already signaled us, is confirmed by the distributions of VD classes, namely an obvious decreasing trend of the IVD towards the poorest differentiated subtype of the group – 5A (Table 14; Figure 14).

Table 14 – *P-values of χ^2 test comparison between distributions of IVD classes in "necrotizing" phenotype group of patterns*

χ^2 test	Gleason 3C	Gleason 4A	General
Gleason 3C			
Gleason 4A	0.314		
Gleason 5A	**0.003**	**<0.0001**	
General			**<0.0001**

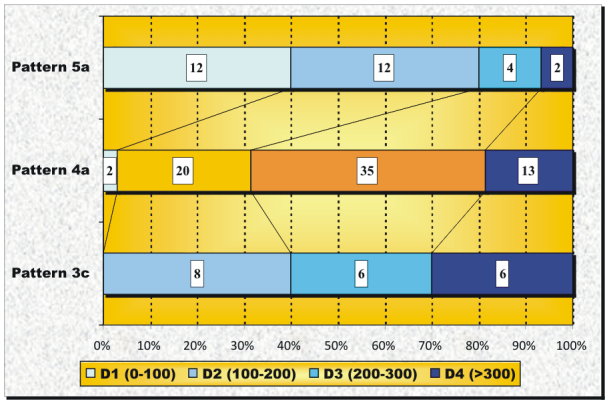

Figure 14 – *Graphic representation of different IVD ratio classes' proportions in "necrotizing" phenotype group of patterns.*

"Solid" phenotype

In "solid" group, there is a clear statistically confirmed difference between IVD distributions of different subtypes (Table 15; Figure 15).

Table 15 – *P-values of K–S test comparison between distributions of IVD values in "solid" phenotype group of patterns*

K–S test	Gleason 3A	Gleason 3B	Gleason 4B
Gleason 3A			
Gleason 3B	**0.0002**		
Gleason 4B	**<0.0001**	**<0.0001**	
Gleason 5B	**<0.0001**	**0.03** (<0.05)	**0.0001**

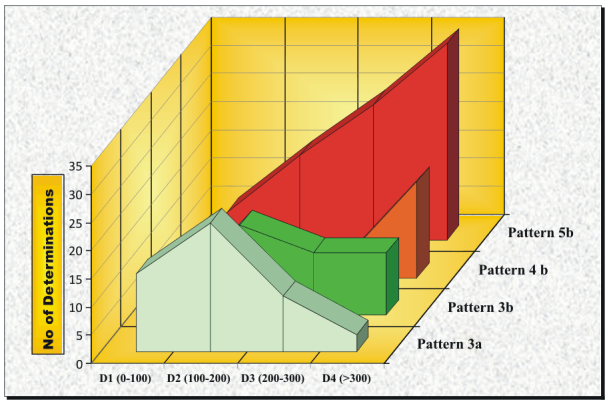

Figure 15 – *Graphic representation of different IVD ratio values distributions in "solid" phenotype.*

The trend of IVD distribution in the subtypes of this group is completely opposite to that of "necrotizing" group, meaning that IVD tends obviously to increase from better differentiated subtype 3A towards poorly differentiated subtype 4B (Table 16; Figure 16).

Table 16 – *P-values of χ^2 test comparison between distributions of IVD classes in "solid" phenotype group of patterns*

χ^2 test	Gleason 3A	Gleason 3B	Gleason 4B	General
Gleason 3a				
Gleason 3b	**0.003**			
Gleason 4b	**<0.0001**	**<0.0001**		
Gleason 5b	**<0.0001**	0.086	**0.009**	
General				**<0.0001**

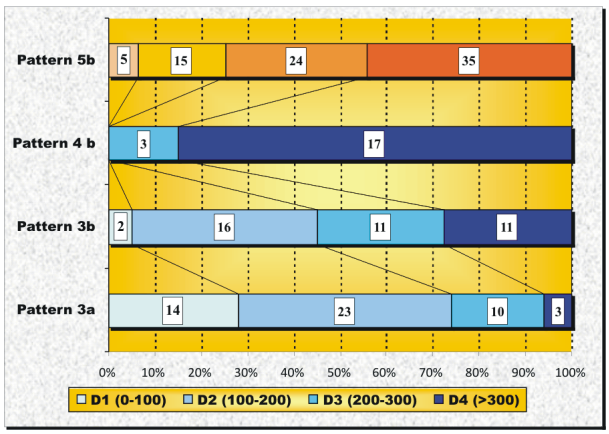

Figure 16 – *Graphic representation of different IVD ratio classes' proportions in "solid" phenotype group of patterns.*

However, in the poorest differentiated subtype – 5B, the vasculature tends to become less dense, with a distribution of IVD classes comparable to that of better differentiated subtype 3B (Table 16; Figure 16).

Conclusions

The intratumoral vascular network showed an overall trend of interstitial densifying, parallel with the decrease of the tumoral degree of differentiation but only up to pattern 4, in pattern 5 presenting a regressive trend. In the defined phenotypes, however, the intratumoral vascular network had two diverging trends. Whereas in "solid" phenotype the evolving pattern of VD related to the degree of differentiation was similar with the one mentioned above and noticed to the general assessment, in "necrotizing" phenotype the vascular network showed a regressive trend parallel to the decrease of tumoral differentiation. These observations open the way to further studies to verify the hypothesis of different cellular populations in prostatic carcinoma with different biologic behavior.

Acknowledgments

This study represents part of the final results of two research projects: No. 255/2003 and No. 445/2004, supported by grant from the Ministry of Education and Research through "VIASAN" Program.

References

[1] Cabanne F, Bonenfant JL, Tumoral stroma. In: Cabanne F, Bonenfant JL, Gagné F, Garneau R *et al.* (eds) *Anatomie pathologique: principes de pathologie générale et spéciale*, Les Presses de L'Université Laval, Québec – Maloine S.A., Editeur, Paris, 1980, 254–257.

[2] Zaharia B, Pleşea IE, Stroma tumorală. În: Zaharia B, Pleşea IE, Foarfă Camelia, Georgescu Claudia Valentina, *Morfopatologie generală*, Ed. Medicală Universitară, Craiova, 2005, 181–182.

[3] Folkman J, *Fundamental concepts of the angiogenic process*, Curr Mol Med, 2003, 3(7):643–651.

[4] Grant DS, Wesley Rose R, Kinsella JK, Kibbey MC, Angiogenesis as a component of epithelial–mesenchymal interactions. In: Goldberg ID, Rosen EM (eds) *Epithelial–mesenchymal interactions in cancer*, Birkhäuser Verlag, Basel–Boston–Berlin, 1995, 235–248.

[5] Schamhart DH, Kurth KH, *Role of proteoglycans in cell adhesion of prostate cancer cells: from review to experiment*, Urol Res, 1997, 25(Suppl 2):S89–S96.

[6] Grossfeld GD, Hayward SW, Tlsty TD, GR Cunha, *The role of stroma in prostatic carcinogenesis*, Endocr Relat Cancer, 1998, 5(4):253–270.

[7] Tuxhorn JA, Ayala GE, Rowley DR, *Reactive stroma in prostate cancer progression*, J Urol, 2001, 166(6):2472–248.

[8] Niu YN, Xia SJ, *Stroma–epithelium crosstalk in prostate cancer*, Asian J Androl, 2009, 11(1):28–35.

[9] Stoiculescu A, Pleşea IE, Pop OT, Alexandru DO, Man M, Serbănescu M, Pleşea RM, *Correlations between intratumoral interstitial fibrillary network and tumoral architecture in prostatic adenocarcinoma*, Rom J Morphol Embryol, 2012, 53(4):941–950.

[10] Pallares J, Rojo F, Iriarte J, Morote J, Armadans LI, de Torres I, *Study of microvessel density and the expression of the angiogenic factors VEGF, bFGF and the receptors Flt-1 and FLK-1 in benign, premalignant and malignant prostate tissues*, Histol Histopathol, 2006, 21(8):857–865.

[11] Folkman J, Cotran R, *Relation of vascular proliferation to tumor growth*, Int Rev Exp Pathol, 1976, 16:207–248.

[12] Folkman J, Watson K, Ingber D, Hanahan D, *Induction of angiogenesis during the transition from hyperplasia to neoplasia*, Nature, 1989, 339(6219):58–61.

[13] Weidner N, Carroll PR, Flax J, Blumenfeld W, Folkman J, *Tumor angiogenesis correlates with metastasis in invasive prostate carcinoma*, Am J Pathol, 1993, 143(2):401–409.

[14] Brawer MK, *Quantitative microvessel density. A staging and prognostic marker for human prostatic carcinoma*, Cancer, 1996, 78(2):345–349.

[15] Lissbrant IF, Stattin P, Damber JE, Bergh A, *Vascular density is a predictor of cancer-specific survival in prostatic carcinoma*, Prostate, 1997, 33(1):38–45.

[16] Carmeliet P, Jain RK, *Angiogenesis in cancer and other diseases*, Nature, 2000, 407(6801):249–257.

[17] Bono AV, Celato N, Cova V, Salvadore M, Chinetti S, Novario R, *Microvessel density in prostate carcinoma*, Prostate Cancer Prostatic Dis, 2002, 5(2):123–127.

[18] Stefanou D, Batistatou A, Kamina S, Arkoumani E, Papachristou DJ, Agnantis NJ, *Expression of vascular endothelial growth factor (VEGF) and association with microvessel density in benign prostatic hyperplasia and prostate cancer*, In Vivo, 2004, 18(2):155–160.

[19] Srivastava A, Laidler P, Davies RP, Horgan K, Hughes LE, *The prognostic significance of tumor vascularity in intermediate-thickness (0.76–4.0 mm thick) skin melanoma. A quantitative histologic study*, Am J Pathol, 1988, 133(2):419–423.

[20] Weidner N, Semple JP, Welch WR, Folkman J, *Tumor angiogenesis and metastasis – correlation in invasive breast carcinoma*, N Engl J Med, 1991, 324(1):1–8.

[21] Dickinson AJ, Fox SB, Persad RA, Hollyer J, Sibley GN, Harris AL, *Quantification of angiogenesis as an independent predictor of prognosis in invasive bladder carcinomas*, Br J Urol, 1994, 74(6):762–766.

[22] Tomisaki S, Ohno S, Ichiyoshi Y, Kuwano H, Maehara Y, Sugimachi K, *Microvessel quantification and its possible relation with liver metastasis in colorectal cancer*, Cancer, 1996, 77(8 Suppl):1722–1728.

[23] Papamichael D, *Prognostic role of angiogenesis in colorectal cancer*, Anticancer Res, 2001, 21(6B):4349–4353.

[24] Sanz-Ortega J, Steinberg SM, Moro E, Saez M, Lopez JA, Sierra E, Sanz-Esponera J, Merino MJ, *Comparative study of tumor angiogenesis and immunohistochemistry for p53, c-ErbB2, c-myc and EGFr as prognostic factors in gastric cancer*, Histol Histopathol, 2000, 15(2):455–462.

[25] Giatromanolaki A, *Prognostic role of angiogenesis in non-small cell lung cancer*, Anticancer Res, 2001, 21(6B):4373–4382.

[26] Strohmeyer D, Strauss F, Rössing C, Roberts C, Kaufmann O, Bartsch G, Effert P, *Expression of bFGF, VEGF and c-met and their correlation with microvessel density and progression in prostate carcinoma*, Anticancer Res, 2004, 24(3a):1797–1804.

[27] Strohmeyer D, Rössing C, Strauss F, Bauerfeind A, Kaufmann O, Loening S, *Tumor angiogenesis is associated with progression after radical prostatectomy in pT2/pT3 prostate cancer*, Prostate, 2000, 42(1):26–33.

[28] Van Moorselaar RJ, Voest EE, *Angiogenesis in prostate cancer: its role in disease progression and possible therapeutic approaches*, Mol Cell Endocrinol, 2002, 197(1–2): 239–250.

[29] van Niekerk CG, van der Laak JA, Börger ME, Huisman HJ, Witjes JA, Barentsz JO, Hulsbergen-van de Kaa CA, *Computerized whole slide quantification shows increased microvascular density in pT2 prostate cancer as compared to normal prostate tissue*, Prostate, 2009, 69(1):62–69.

[30] Arakawa A, Soh S, Chakraborty S, Scardino PT, Wheeler TM, *Prognostic significance of angiogenesis in clinically localized prostate cancer (staining for Factor VIII-related antigen and CD34 Antigen)*, Prostate Cancer Prostatic Dis, 1997, 1(1): 32–38.

[31] Gyftopoulos K, Vourda K, Sakellaropoulos G, Perimenis P, Athanasopoulos A, Papadaki E, *The angiogenic switch for vascular endothelial growth factor-A and cyclooxygenase-2 in prostate carcinoma: correlation with microvessel density, androgen receptor content and Gleason grade*, Urol Int, 2011, 87(4):464–469.

[32] Montironi R, Galluzzi CM, Diamanti L, Taborro R, Scarpelli M, Pisani E, *Prostatic intra-epithelial neoplasia. Qualitative and quantitative analyses of the blood capillary architecture on thin tissue sections*, Pathol Res Pract, 1993, 189(5): 542–548.

Corresponding author
Iancu Emil Pleşea, Professor, MD, PhD, Department of Pathology, University of Medicine and Pharmacy of Craiova, 2 Petru Rareş Street, 200349 Craiova, Romania; Phone +40251–306109, e-mail: pie1956@yahoo.com

Received: December 10th, 2012

Accepted: April 20th, 2013